Catalysis Today 172 (2011) 152–157

Contents lists available at ScienceDirect

Catalysis Today

journal homepage: www.elsevier.com/locate/cattod

Study of the effect of cobalt content in obtaining olefins and paraffins using the Fischer-Tropsch reaction

Bianca Viana de Sousa[a,*], Meiry Gláucia Freire Rodrigues[a], Leonardo Andrés Cano[b], Maria Virginia Cagnoli[b], José Fernando Bengoa[b], Sérgio Gustavo Marchetti[b], Gina Pecchi[c]

[a] UFCG/CCT/UAEQ/LABNOV, Campina Grande, Paraíba, Brazil
[b] CINDECA/UNLP/FCE, Calle 47 No 257, 1900 La Plata, Argentina
[c] Facultad de Ciencias Químicas, Universidad Concepción, Concepción, Chile

ARTICLE INFO

Article history:
Received 29 November 2010
Received in revised form 9 February 2011
Accepted 14 February 2011
Available online 31 March 2011

Keywords:
Catalysis
MCM-41
Cobalt
Fischer-Tropsch

ABSTRACT

This work presents the synthesis, characterization and testing of catalysts for the Fischer-Tropsch reaction. Molecular sieve MCM-41 was prepared under hydrothermal treatment at 150 °C for 2 days, using the following molar composition of reagents: 1 SiO_2:0.27 CTABr:0.19 TMAOH:40 H_2O. Obtaining the mesoporous molecular sieve, Si-MCM-41, was confirmed by X-ray diffraction. The deposition of cobalt on MCM-41 support was carried out by wet impregnation, using an aqueous solution of cobalt nitrate. The images obtained from TEM clearly showed a good dispersion of the cobalt on the support (MCM-41). The textural characteristics of the samples were investigated by isothermal gas adsorption/desorption. Using the BJH method, it was possible to obtain the values of the average pore diameter on adsorption and desorption. The obtained catalysts containing different cobalt concentrations were evaluated for the Fischer-Tropsch reaction. Increasing the temperature increases the selectivity to olefins with the 15 wt.% Co/MCM-41 catalyst, as well as increases the selectivity to methane with the 5 wt.% Co/MCM-41 catalyst.

1. Introduction

The Fischer-Tropsch synthesis (FTS) is a key industrial process for producing high quality liquid fuels, paraffins, alcohols and other value-added products using abundant and renewable sources such as natural gas and biomass [1,2]. This process consists of converting synthesis gas (CO and H_2 mixture) into long-chain hydrocarbon [3,4].

Other factors that make the use of this technology, from natural gas, interesting are the large existing reserves, the need to monetize remote or stranded natural gas, the low quality of crude oil, and the modern environmental specifications that have become very restricted [3,5].

Cobalt and iron catalysts have found industrial application in this process, for example, Sasol (Qatar). However, cobalt catalysts are preferred for the FTS process due to their low activity in the reaction of water–gas displacement, low deactivation and a high yield of linear paraffins with regard to iron catalysts [6–9]. When these catalysts are used in low reaction temperatures, this leads to high selectivity of branched-chain paraffins which are desirable as they are precursors of synthetic diesel [4,7].

Supported Co-based catalysts have been widely used to achieve high yields of paraffinic hydrocarbons in FT synthesis. Some papers published so far have focused on elucidating the roles of support and its porosity in reaction rate and product selectivity in the Co-catalyzed synthesis and suggested, for example, different degrees of metal dispersion and catalyst reduction, consequent different behaviors of CO and H_2 adsorption on Co particles, mass transport limitations for CO and hydrocarbons in catalyst pores, and pore filling by condensation of heavier hydrocarbons formed [9].

Commercially applied catalysts are based on high levels of cobalt (15–30 wt.%) supported on porous inorganic oxides with a high surface area such as silica, alumina, titanium so as to obtain higher dispersion of the metal [4,8].

Optimizing the particle size, dispersion and reducibility of cobalt is one of the greatest challenges in preparing these catalysts so as to make them efficient in the FTS [4]. It is known that the smaller the particle size of cobalt, the stronger the interaction between cobalt and the support is. This interaction causes both diminished reducibility and activity for the FTS [4,6,8].

The Co components are usually supported on SiO_2, Al_2O_3, and TiO_2 with microporous and mesoporous structures. Mesoporous molecular sieves recently developed, such as MCM-41, FSM-16 and SBA-15, have well-defined periodic mesopores, consequently provide very narrow pore size distributions, and possess large pore

* Corresponding author. Tel.: +55 83 2101 1117; fax: +55 83 2101 1114.
E-mail address: bianca@deq.ufcg.edu.br (B.V.d. Sousa).

0920-5861/$ – see front matter © 2011 Elsevier B.V. All rights reserved.
doi:10.1016/j.cattod.2011.02.035

volumes of 1–2 cm^3/g and high surface areas reaching 1000 m^2/g. The supported metal catalyst show enhanced thermal stability due to interaction between the active metal and support which leads to a decrease in sintering and an extended catalyst life. But also the utilization of such novel materials as supports of Co catalysts may make it possible to design new catalysts with higher productivity for C10–C20 paraffin as the main component of diesel oil [10–12].

Thus, the analysis of the literature suggests that in order for cobalt catalysts to be efficient in the FTS, it is necessary to have high density of the active sites; desirable distribution of the metal on the catalyst surface (especially in the fixed bed reactor); metal particles of cobalt larger than 6–8 nm; a low fraction of poorly reduced compounds (silicate of cobalt, cobalt aluminate, etc.); the metallic surface and the structure of the catalyst must be stable under the reaction conditions [4,10].

The Fischer-Tropsch reaction produces a wide spectrum of hydrocarbons and oxygenated products the formation of which can be controlled by kinetic and mechanistic factors. In the last 30 years or so, many studies on the Fischer-Tropsch synthesis have focused on the dependence of the length of the hydrocarbon chain [13]. The intrinsic kinetics that is characteristic of FTS is a gradual growth of the chain similar to a polymerization of CH_2– groups on the surface of the catalyst. This is valid regardless of the products that are formed, paraffins, olefins or oxygenated compounds [14].

Both the olefins and the paraffins follow the Schulz-Flory distribution. This distribution determines a relationship between product yield and the number of carbons, i.e., increasing the length of the chain, thus showing selectivity from waxes to gases [15].

This study sets out to evaluate the production of olefins and paraffins using Co/MCM-41-type catalysts with different levels of metal contents in Fischer-Tropsch synthesis.

2. Experimental

2.1. Synthesis of MCM-41

The method used is based on the work of Cheng et al. [16]. The preparation of the molecular sieve, MCM-41, consisted of the following steps: TMAOH and CTABr was added to deionized water at 50 °C under agitation, this condition being maintained until the solution was homogenized; after cooling to room temperature, fumed silica was added to the reaction medium, and the solution stirred for a further 2 h. After this time, the reaction mixture was subjected to ageing for 24 h. The final product was obtained after autoclaving for 2 days at 150 °C, followed by washing, drying, and calcination to remove the surfactant, under nitrogen flow, from room temperature to 540 °C at a heating ramp rate of 5 °C/min with a flow rate of 100 mL/g_{cat} min and, under a synthetic air flow, it remained at this temperature (540 °C), for 6 h. The sample was synthesized with the following molar composition: 1 SiO_2:0.27 CTABr:0.19 TMAOH:40 H_2O.

2.2. Preparation of the Co/MCM-41 catalyst

The deposition of metal with 5 and 15 wt.% Co on MCM-41 support was performed by wet impregnation, using an aqueous solution of 0.1 M cobalt nitrate ($Co(NO_3)_2{\cdot}6H_2O$), stirring continuously at room temperature for 30 min. The mixture was then dried at 100 °C for 24 h. The solid material was submitted to the calcination process which, under a nitrogen flow rate of 100 mL/g_{cat} min, from room temperature to 200 °C with a heating ramp of 5 °C/min and kept at this temperature for 1 h. After this period, the nitrogen flow was replaced by synthetic air and the sample heated at 5 °C/min from 200 to 450 °C and kept at this temperature for 2 h.

2.3. Characterization

2.3.1. X-ray diffraction (XRD)

Powder diffraction patterns were measured on a Shimadzu XRD 6000. Operational conditions: Copper Kα radiation at 40 kV/30 mA, a goniometer velocity of 2°/min and a step of 0.02° over the range of 2θ from 2° to 45°. The average diameter of crystallites of the samples studied was determined by the so-called Scherrer equation.

2.3.2. X-ray energy dispersion spectrophotometer (EDX)

The elemental analysis for Si, Al, Ni, Ti, Fe, S, Ca, Zr all of which elements can be present in the catalyst, was performed using an X-ray energy dispersion spectrophotometer (EDX-700 Shimadzu).

2.3.3. Nitrogen adsorption (BET method)

The textural characteristics of the samples analysed were investigated by isothermal gas adsorption/desorption of N_2 at −196 °C using ASAP 2020 equipment. The adsorption and desorption isotherms of N_2 were obtained in the range of relative pressure (P/P_0) between 0.02 and 1.0. The values of the average pore diameter and surface area (S_{BET}) were obtained by the method proposed (BET). Using the *t*-plot method, and the Harkins-Jura correlation of thickness, the external surface area (S^{ext}) and the volume of pores (V_P) were measured. The measurement of the total surface area was determined by the single-point method at $P/P_0 \approx 0.10$–0.25 [17] and as to the total pore volume (V_p^{total}), the single-point method $P/P_0 \approx 0.977$ was applied. Using the BJH method, it was possible to obtain the values of the average pore diameter on adsorption and desorption.

2.3.4. Transmission electron microscopy (TEM)

The analyses were performed on JEOL equipment Model JEM-1200 EX II Instrument With the technique of embedding in Araldite resin and then cut with Sorvall MT 5000 ultramicron.

2.4. Catalytic tests

Before the catalytic tests, in order to obtain the metallic function, 400 mg of the catalyst were reduced in situ in a fixed bed reactor under a flow of hydrogen at 500 °C for 5 h. Catalyst activity and selectivity were evaluated out in a stainless steel fixed bed flow microreactor operating by 92 h of catalyst time on stream (TOS), with the first 50 h being at a reaction temperature of 270 °C and the remaining 42 h at that of 350 °C at a total pressure of 1 atm. Hydrogen and carbon monoxide were fed to the reactor at a molar feed ratio of 2:1. Analysis of the products of reaction was performed by "on-line" gas chromatography using a KONIK KNK3000HRGC chromatograph with a flame ionizer detector (FID) and thermal conductivity (TCD) and a Spectra-Physics SP 4290 electronic integrator, which evaluates the peak areas obtained automatically. A 30 m GS-alumina capillary column PLOT (J&W Scientific) was used.

3. Results and discussion

3.1. X-ray energy dispersion spectrophotometer (EDX)

It can be seen from the results in Table 1 that the samples under study had high levels of silica (SiO_2), given that the structure of the molecular sieve consists solely of silica. It is observed that the synthesized MCM-41 showed an appreciable level of bromine in its composition, indicating the presence of the surfactant so as shape the mesoporous structure. It was found that the calcination process used to remove the surfactant was effective, since 99% of the level shown to be present in the sample synthesized was eliminated. After the process of impregnating cobalt on MCM-41 with nominal

Table 1
Chemical composition of the samples of synthesized MCM-41, calcined MCM-41 and the catalysts with 5 and 15 wt.% Co/MCM-41 in the form of oxides and in the form of elements for cobalt.

Sample	SiO_2	Br	Co_2O_3	Co	Impurities
MCM-41 synthesized	74.5	24.9	–	–	0.60
MCM-41 calcined	99.5	0.15	–	–	0.35
5 wt.% Co/MCM-41	90.2		8.9	6.34	0.9
15 wt.% Co/MCM-41	77.8		21.5	15.31	0.7

Table 2
Results of average sizes of crystallite obtained of the catalysts 5 and 15 wt.% Co/MCM-41 via X-ray diffraction.

Catalysts	Average particular size (nm)
5 wt.% Co/MCM-41	44.2
15 wt.% Co/MCM-41	47.3

levels ranging 5 and 15 wt.% Co, it was possible to verify the presence of cobalt oxide (Co_2O_3) in the samples. Analyzing the data of cobalt in the form of elements, one can see that the percentage of cobalt is obtained close to the desired value (5 and 15 wt.%).

3.2. X-ray diffraction (XRD)

That a mesoporous molecular sieve, Si-MCM-41 was obtained can be confirmed by X-ray diffractogram, shown in Fig. 1. A check was made that the procedure for removing the occluded surfactant (calcination) did not affect the structure of the MCM-41 synthesized, as the peaks corresponding to the hexagonal phase were maintained. It should also be noted also that for the sample calcined, an increase occurs in the intensity of the diffraction peaks and their displacement to larger angles.

It is observed from Fig. 2a that the mesoporous structure remained intact after the treatments of impregnation and calcination of the catalysts for 5 and 15 wt.% Co. In Fig. 2, the characteristic peaks of cobalt oxide, formed from the decomposition of salt ($Co(NO_3)_2{\cdot}6H_2O$) on the mesoporous molecular sieve MCM-41 after calcination, are delicately attenuated in terms of intensity, in relation the major peaks between $2\theta = 20^\circ$ and 80°.

The crystalline phases were identified using the ICDD-JCPDS library (International Center for Diffraction Data), where the cards are available for various materials crystallographic. We observed the presence of a mixture of oxides and Co_2O_3 and Co_3O_4. The peaks identified based on the ICDD-JCPDS were: Co_2O_3 ($2\theta = 22.97, 31.26$) and Co_3O_4 ($2\theta = 36.75, 44.82; 59.38; 65.14$).

Table 2 presents the results of average sizes of crystallites of the catalysts studied, which were calculated by the XRD-6000 v4.1 crystallite program, based on the Scherrer equation. The mean diameters of the crystallites were obtained through the most intense reflections of each phase, and the final average diameter was calculated by the arithmetic mean of the diameters obtained for each reflection.

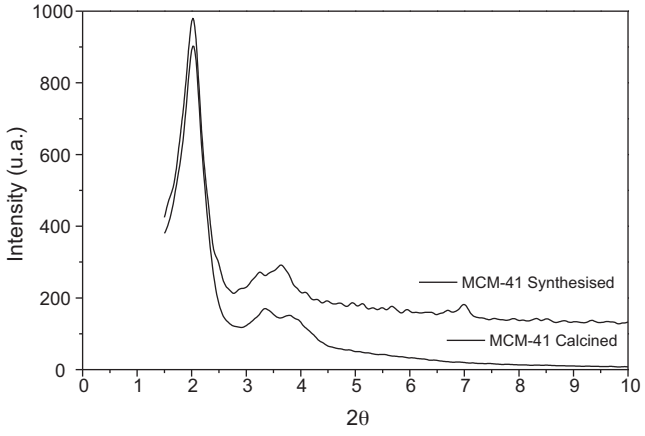

Fig. 1. Diffractogram of the samples synthesised and calcined MCM-41.

3.3. Nitrogen adsorption (BET method)

The isotherms of adsorption/desorption of N_2 presented in Fig. 3 of the calcined MCM-41 sample are type IV, relative to the mesoporous materials [18]. Three regions can be distinguished: the first, given to low relative pressures ($P/P_0 < 0.2$) corresponds to the adsorption of N_2, in the monolayer; the second, the inflection given to $P/P_0 = 0.4$–0.6, the capillary condensation occurs that is characteristic of mesoporous materials; the third, ($P/P_0 > 0.9$), can be attributed to adsorption of the multilayers of the external surface [19,20]. The desorption curve showed a hysteresis loop of the H_2 type to partial pressures (P/P_0) between 0.4 and 0.6. This

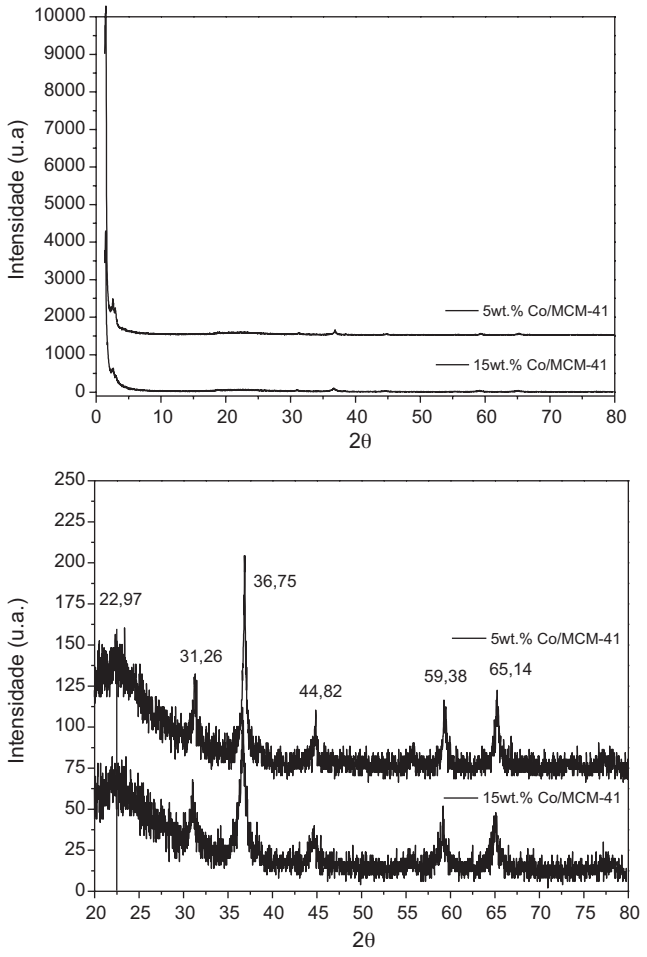

Fig. 2. Diffractogram of the catalyts (a) in scale of 1.3 at 80° and (b) scale of 20 at 80° after the impregnation and calcination.

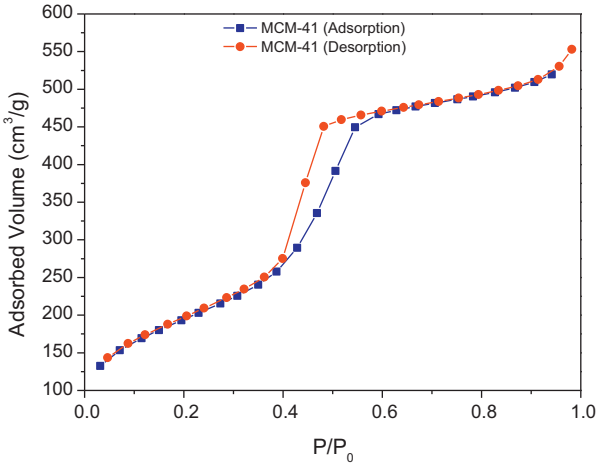

Fig. 3. Adsorption–desorption isotherms of N_2 at −196 °C of the calcined MCM-41 sample.

behavior corresponds to porous materials consisting of cylinders open at both ends [21,22].

The isotherms of adsorption/desorption of N_2 for the 5 and 15 wt.% Co/MCM-41 catalysts (Fig. 4) showed similar profiles typically of the type IV. The desorption curves for these catalysts showed a hysteresis loop of type H_2 partial pressures (P/P_0) between 0.4 and 0.6 that can be attributed to the capillary condensation and evaporation in the mesoporous interiors of the tubes [17,23].

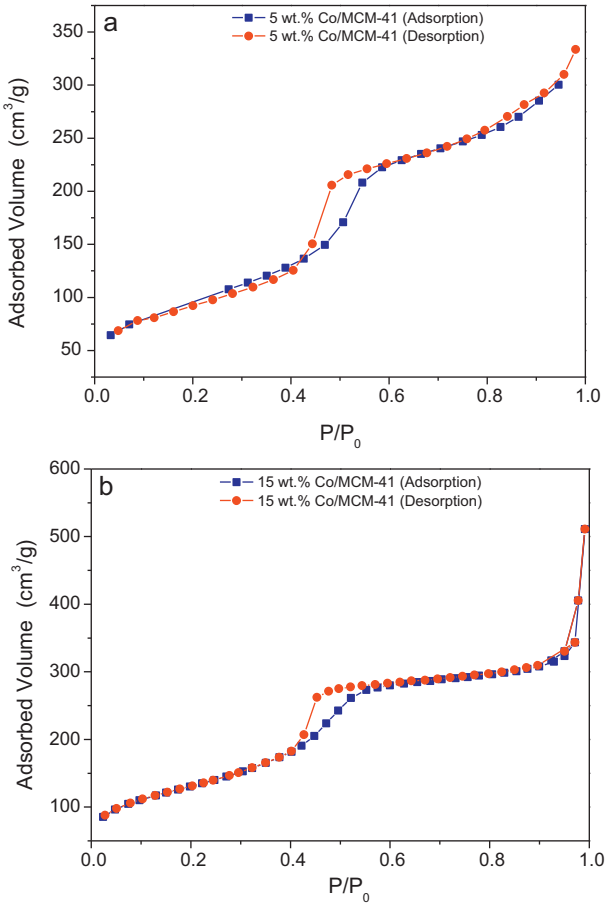

Fig. 4. Adsorption–desorption isotherms of N_2 at −196 °C catalyst of (a) 5 wt.% Co/MCM-41 and (b) 15 wt.% Co/MCM-41.

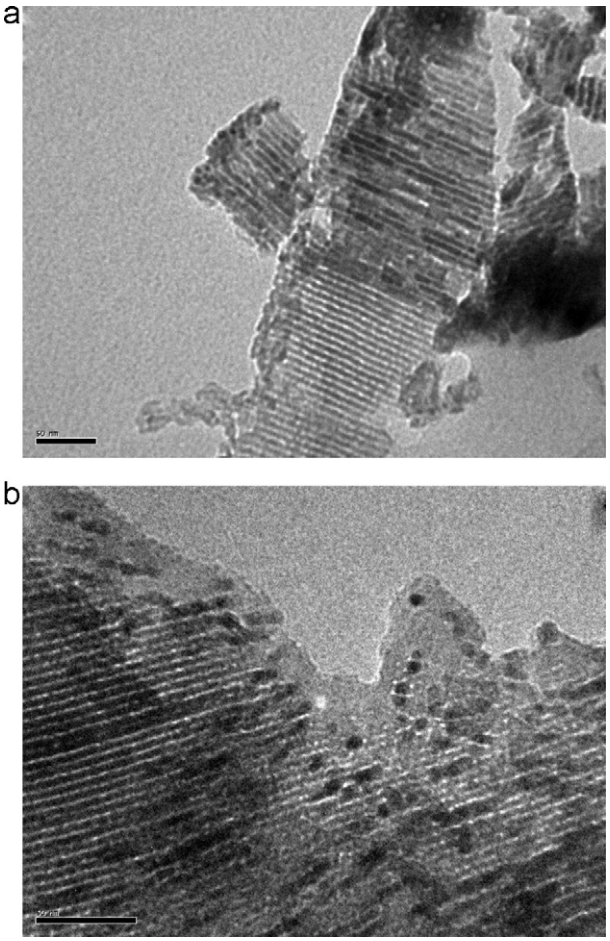

Fig. 5. Micrographs of the catalysts (a) 5 wt.% Co/MCM-41 and (b) 15 wt.% Co/MCM-41.

According to the evaluation of specific area using the BET method presented in Table 3, it is verified that the catalyst with 15 wt.% Co/MCM-41 after impregnation and calcination process, presented specific surface area (S_{BET}) and total pore volume (V_p) greater than the catalyst with 5 wt.% Co/MCM-41. This fact can be attributed to dispersion of cobalt oxide particles on the surface of the MCM-41 as well as the very porous structure of these oxides. It was observed that the values of the external area is 11–15% of the specific surface area indicating the porous nature of these materials and higher presence of mesopores in the catalyst with 15 wt.% Co/MCM-41 [18,24].

3.4. Transmission electron microscopy (TEM)

It can be seen in the micrograph (Fig. 5) of the catalyst 5 wt.% Co/MCM-41 that channels are homogeneous and that the cobalt particles are well dispersed inside the channels. Catalyst for the 15 wt.% Co/MCM-41 it clearly within the dark areas of the channels corresponding to particles of cobalt. The sizes of these particles are clearly larger than the channels. This fact indicates that these particles must be out of the channels making the system more heterogeneous. The activation process (calcination and reduction) in the catalysts (5 and 15 wt.% Co/MCM-41) did not affect the mesoporous structure of the same. The catalysts showed regular hexagonal arrangement evident.

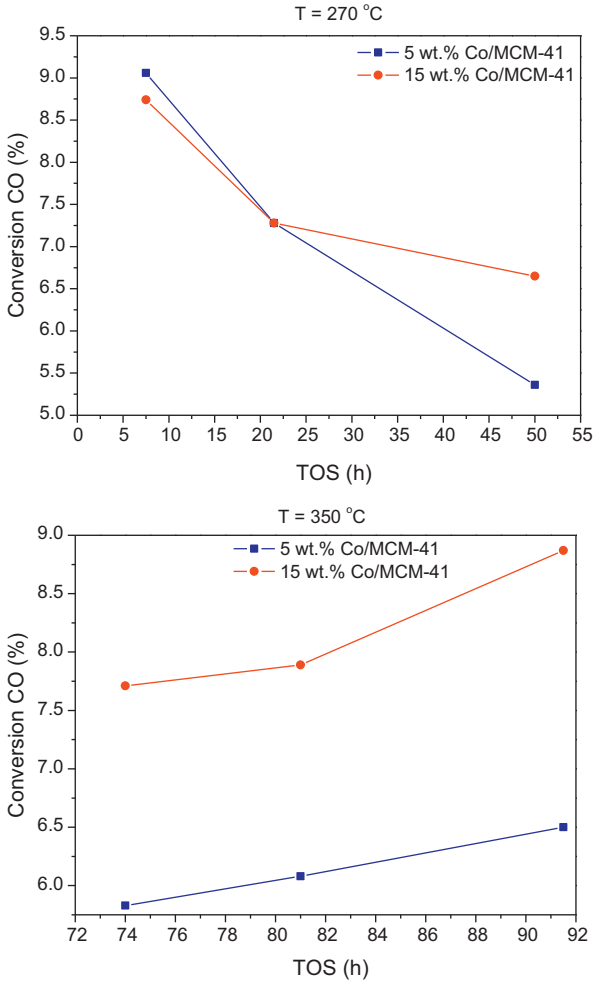

Fig. 6. Curve of CO conversion (%) of the catalysts 5 and 15 wt.% Co/MCM-41 in $T = 250\,^{\circ}C$ (a) and $T = 350\,^{\circ}C$ (b).

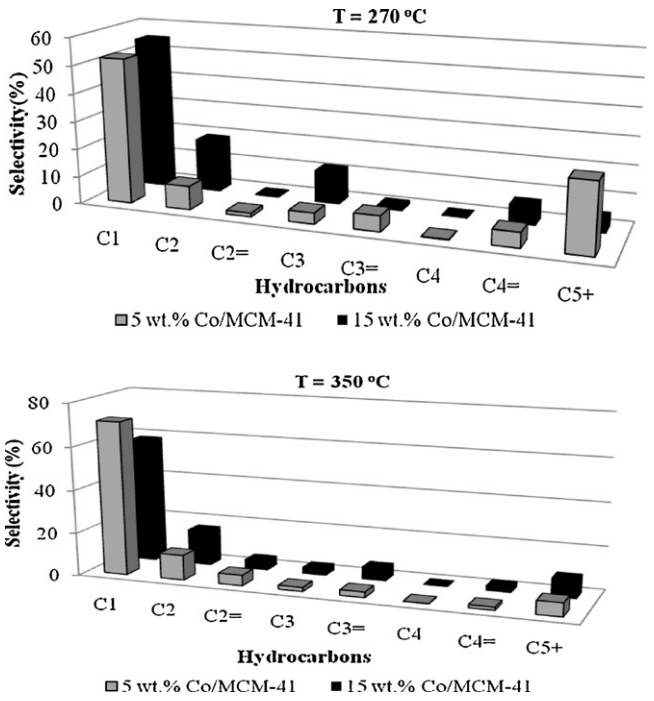

Fig. 7. Paraffins and olefins formed for 21.5 and 81 h of its time on stream (TOS) at temperatures of 270 and 350 °C, respectively, of the catalysts 5 and 15 wt.% Co/MCM-41.

3.5. Catalytic test

Fig. 6 (a and b) shows the curves of CO conversion as function of time on stream (TOS) of the Co/MCM-41 catalysts. It can be observed that the CO conversion rates for the catalyst with 5 wt.% Co/MCM-41 was higher than for the catalyst 15 wt.% Co/MCM-41 when the reaction reached a pseudo-steady state (7.5 h), but hydrocarbon formation was slightly higher for the catalyst 15 wt.% Co/MCM-41. This can be attributed to the greater number of active sites present in this catalyst (15 wt.% Co/MCM-41).

Analyzing the data in Table 4 it is observed that the catalyst 5 wt.% Co/MCM-41 up to 21.5 h of reaction showed selectivity to methane less than 15 wt.% Co/MCM-41 catalyst. The increase in temperature favored the selectivity to methane with the 5 wt.% Co/MCM-41 catalyst while the methane selectivity for the 15 wt.% Co/MCM-41 catalyst remained almost the same. Similar results were found by Khodakov et al. [8] using molecular sieves (MCM-41) with different pore sizes, and observed that independent of the pore size of the supported catalysts showed high selectivity to methane. Duvenhage and Coville [25] reported their studies of cobalt catalysts supported on TiO_2 and SiO_2, also tend to be selective to methane.

It is observed that the catalysts studied showed opposite behavior in relation to ratio of olefin/paraffin since, with increasing

Table 3
Textural analysis of samples: MCM-41 calcined, 5 and 15 wt.% Co/MCM-41.

Samples	S_{BET} (m^2/g)	S^{ext} (m^2/g)	V_p^{total} (cm^3/g)	D_p (nm)
MCM-41 calcined	693	81	0.78	0.49
5 wt.% Co/MCM-41	349	160	0.45	0.37
15 wt.% Co/MCM-41	476	70	0.80	0.66

Table 4
Selectivity to methane and the ratio of olefins and paraffins formed as a function of reaction time for catalysts 5 and 15 wt.% Co/MCM-41.

Temperature (°C)	270			350		
5 wt.% Co/MCM-41 catalyst						
TOS (h)	7.5	21.5	50	74	81	91.5
Olefins/paraffins	0.64	0.79	0.59	0.54	0.56	0.54
Methane (%)	45.1	52.2	63.8	73.2	71.4	67.6
15 wt.% Co/MCM-41 catalyst						
TOS (h)	7.5	21.5	50	74	81	91.5
Olefins/paraffins	0.18	0.20	0.22	0.55	0.52	0.48
Methane (%)	47.9	55.1	58.4	52.7	58.3	51.4

temperature this ratio increased for the catalyst with 15 wt.% Co/MCM-41, indicating that the formation of olefins was favored while for the catalyst 5 wt.% Co/MCM-41 that reason declined. These results are characteristic of the presence of constraints of transport and secondary reactions. Iglesia et al. [26] showed that the limitations of transportation of hydrocarbons on the production of paraffins and olefins follows two paths. First, only hydrocarbons are formed by secondary reactions due to the low reactivity of alkanes. Second, the diffusivity of hydrogen is higher than that of CO; reason H_2/CO increases with porosity and promotes the production of saturated molecules. The importance of secondary reactions depends on the density of active sites and diffusional restrictions caused by the products in the pores of the catalyst. The importance of secondary reactions depends on the density of active sites and diffusional restrictions caused by the products in the pores of the catalyst. Another factor to consider is the size of metal particles [6,10]. Fig. 7 shows the amount of paraffins and olefins formed in times on stream of 21.5 h and 81 h at temperatures of 270 °C and 350 °C, respectively, for the catalysts 5 and 15 wt.% Co/MCM-41.

4. Conclusions

A combination of techniques (XRD, BET, TEM) showed that the MCM-41 have a structure that includes multi-level mesopores, crystallites and grains within the original particles.

According to the results of EDX, the cobalt incorporated into the support (MCM-41) were close to theoretical values, demonstrating the efficiency of wet impregnation.

The TEM images clearly showed the presence of well dispersed particles of cobalt in the 5 and 15 wt.% Co/MCM-41 catalysts. The high selectivity to methane observed in the cobalt catalyst was attributed to low reducibility of small cobalt particles and the diffusion limitations of CO in the pores of the catalyst. The results show that increasing the temperature increases the selectivity to olefins with the 15 wt.% Co/MCM-41 catalyst, as well as increases the selectivity to methane with the 5 wt.% Co/MCM-41 catalyst.

Acknowledgement

The authors are gratefully acknowledged to the PRH-25/ANP/MCT.

References

[1] R. Ravishankar, M.M. Li, A. Borgna, Catal. Today 106 (2005) 149–153.
[2] O. Ducreux, B. Rebours, J. Lynch, M. Roy-Auberger, D. Bazin, Oil Gas Sci. Technol.-Rev. IFP 64 (1) (2009) 49–62.
[3] M.E. Dry, Catal. Today 71 (2002) 227–241.
[4] F. Diehl, A.Y. Khodakov, Oil Gas Sci. Technol.-Rev. IFP 64 (2009) 11–24.
[5] A.C. Vosloo, Fuel Process. Technol 71 (2001) 149–155.
[6] H. Xiong, Y. Zhang, K. Liew, J. Li, J. Mol. Catal. A: Chem. 295 (2008) 68–76.
[7] E. Iglesia, Appl. Catal. A 161 (1997) 59–78.
[8] Y. Khodakov, A. Griboval-Constant, R. Bechara, V.L. Zholobenko, J. Catal. 206 (2002) 230–241.
[9] S. Storsæter, Ø. Borg, E.A. Blekkan, A. Holmen, J. Catal. 231 (2005) 405–419.
[10] G. Prieto, A. Martínez, R. Murciano, M.A. Arribas, Appl. Catal. A 367 (2009) 146–156.
[11] Y. Ohtsuka, Y. Takahashi, M. Noguchi, T. Arai, S. Takasaki, N. Tsubouchi, Y. Wang, Catal. Today 89 (2004) 419–429.
[12] A.M. Saib, M. Claeys, E. van Steen, Catal. Today 71 (2002) 395–402.
[13] J. Patzlaff, Y. Liu, C. Graffmann, J. Gaube, Appl. Catal. A 186 (1999) 109–119.
[14] A.A. Adesina, Appl. Catal. A 138 (1996) 345–367.
[15] J.M. Schweitzer, J.C. Viguié, Oil Gas Sci. Technol.-Rev. IFP 64 (1) (2009) 63–77.
[16] C.-F. Cheng, D. Ho, J. Klinowski, J. Chem. Soc. 93 (1997) 193–197.
[17] M. Kruk, M. Jaroniec, Chem. Mater. 13 (2001) 3169–3183.
[18] G. Leofanti, M. Padovan, G. Tozzola, B. Venturelli, Catal. Today 41 (1998) 207–219.
[19] R. Schmidt, M. Stocker, E. Hansen, D. Akporiaye, O.H. Ellestad, Micropor. Mesopor. Mater. 3 (1995) 443–448.
[20] S. Suvanto, T.A. Pakkanen, J. Mol. Catal. 164 (2000) 273–280.
[21] P. Selvam, S.K. Bathia, C.G. Sonwane, Ind. Eng. Chem. Res. 40 (2001) 3237–3261.
[22] A.Y. Khodakov, V.L. Zholobenko, R. Bechara, D. Dominique, Micropor. Mesopor. Mater. 79 (2005) 29–129.
[23] M. Selvaraj, K. Lee, K.S. Yoo, T.G. Lee, Micropor. Mesopor. Mater. 81 (2005) 343–355.
[24] M.M. Mohamed, N.S. Goma, M. El-Moselhy, N.A. Eissa, J. Colloid Interface Sci. 259 (2003) 331–337.
[25] D.J. Duvenhagen, N.J. Coville, Appl. Catal. A 153 (1997) 43–67.
[26] E. Iglesia, S.C. Reyes, R.J. Madon, S.L. Soled, Adv. Catal. 39 (1993) 221–302.